



## Original Research Article

### Optimization of the Cutting Process Parameters of Ti-6Al-4V Alloy using Hybrid Approach

**\*Olodu, D.D. and Ihenyen, O.I.**

Department of Production Engineering, Faculty of Engineering, University of Benin, PMB 1154, Benin City, Nigeria.

\*dickson.olodu@eng.uniben.edu; imevbore.ihenyen@uniben.edu

#### ARTICLE INFORMATION

##### Article history:

Received 04 October, 2018

Revised 01 November, 2018

Accepted 06 November, 2018

Available online 30 December, 2018

##### Keywords:

Central composite design

FEA model

Hybrid model

Response surface methodology

ANOVA

#### ABSTRACT

*The prediction of machining conditions for minimum cutting forces plays a very important role in machining stability, tool life and residual stresses. In this research, a series of simulations were run in order to evaluate the effect of cutting variables and optimize the cutting conditions to obtain lower cutting force for orthogonal cutting of titanium alloy (Ti-6Al-4V). A predictive Lagrangian-FEA model based on finite element method (FEM) which involved Johnson-Cook material model and fracture criterion was used to simulate chip shapes and cutting forces. The simulation runs plan was designed and carried out based on the central composite design (CCD). A mathematical linear model in terms of cutting speed and feed rate was developed for cutting force using FEA and optimized using response surface methodology (RSM). An optimum cutting force of 1165.04N was obtained at a cutting speed of 70m/min. and a feed rate of 0.21m/rev. The validity of the model shows that a coefficient of determination of 98% and adjusted coefficient of 97% were obtained. Finally, the simulation runs performed to verify the fitted model shows that its adequacy is within 95% prediction interval.*

© 2018 RJEES. All rights reserved.

## 1. INTRODUCTION

Besides high cutting temperatures and chemical reactivity of titanium alloys during machining, cutting tools also suffer from high mechanical pressure and high dynamic loads which result in plastic deformation and rapid tool wear (Olodu, 2018). Therefore, various empirical, mechanistic, analytical and numerical techniques have been applied to model the cutting forces. The empirical modeling is widely used in the absence of other meaningful models. Empirical models often utilize statistical methods and they are only valid for some of the experiments conducted (Olodu, 2018). This technique is based on designed experiments for varying process inputs and measuring process outputs such as cutting forces, surface roughness and tool-

life. For this reason, this method utilizes heavy experimentation at different cutting conditions and it is very costly (Kilickap and Huseyinoglu, 2011).

However, with the development of the digital computer industry, the finite element method (FEM) was widely used to understand the chip formation mechanism in multi-physics scale (Özel and Sima, 2010). In the early decades, FEM couldn't be proven to be fully capable of analyzing practical machining processes. One reason for that was the tendency of many researchers to write their own FEM codes that can handle a specific case which is, mostly, orthogonal cutting (Sasahara, 2005; Sartkulvanich and Altan, 2016; Strenkowski and Moon 2017). Even the researchers who used commercial FEM codes couldn't analyze the practical three-dimensional cutting operations such as ball end milling and drilling because those codes still needed further development to handle such complicated operations (Miller and Bieler, 1999). Another reason for the limitations of FEM in handling practical metal cutting operations is the lack of material property data (flow stress) at the high strains, strain rates and temperatures encountered in metal cutting (Attanasio and Ceretti, 2017). Many researchers used flow stress data that made their FEM results questionable (Stevenson and Wright, 1983). Sima and Özel (2010) modelled the flow stress in the primary deformation zone in FEM as a function of strain rate at room temperature. Umbrello (2018) assumed the flow stress to be a function of strain alone in metal cutting FEM simulations.

Nevertheless, in recent years many successful works were reported in analyzing certain work materials such as titanium alloys by using FEM. In the case of flow stress modeling, Attanasio and Ceretti (2017) used Oxley's parallel-sided shear zone theory to model orthogonal milling. They modified the Johnson-Cook material model by inverse analysis and demonstrated applications in numerous materials. Özel and Sima (2010) also utilized Oxley's analysis to calculate flow stress at high strain rates. By combining data from orthogonal machining with Smooth Particle Hydrodynamics (SPH) experiments, a Johnson-Cook material model was obtained for AISI 1045 steel, Al 6082-T6 aluminium, and titanium alloy Ti6Al4V. More recently, Strenkowski and Moon (2017) used experimental measurements of chip morphology and cutting force in a Levenberg-Marquardt search algorithm to identify the Johnson Cook parameters for high speed machining. Moreover, the strain softening was identified by carrying out torsion tests at high temperature on pure Aluminium (Kilickap and Huseyinoglu, 2011) and on different AlMgSi alloys (Calamaz and Limido, 2016). Sartkulvanich and Altan (2016) confirm that for pure aluminium, the peak stress was reached at strains less than 0.5. Increasing the strain further resulted to a gradual material softening before a relatively constant level was reached. This type of flow stress-strain curves had also been obtained for Ti-6Al-4V titanium alloy (Miller and Bieler, 1999). Ozel and Sima (2010) predicted the residual stresses using a 3D finite element model for machining Ti6Al4V and IN100 nickel-based alloys. Calamaz and Limido (2016) used the Smooth Particle Hydrodynamics (SPH) method in LS-DYNA software to obtain serrated chip formation for orthogonal cutting of titanium alloy (Ti6Al4V), and compared the results with experimental data. Also, the formation of shear localized chips in the cutting of titanium alloy (Ti6Al4V) had been simulated by using elastic-visco-plastic FEM with a modified material model using commercial FEM programs (Sima and Özel 2010).

This study focused on the optimization of the cutting process parameters of Ti-6Al-4V alloy by using hybrid approach (FEA model and response surface methodology) to model the effects of cutting parameters on the main cutting force of Ti6Al4V alloy when orthogonal cutting. This approach tends to decrease the expense of modeling compared to the conventional methods.

## **2. MATERIALS AND METHODS**

### **2.1. Numerical Model of Orthogonal Machining**

The commercial FEA software DEFORM-2DTM, a Lagrangian implicit code, was used to simulate the orthogonal cutting process of Ti6Al4V Titanium alloy (Umbrello, 2018). FEM model of the orthogonal

cutting process was developed and composed of the workpiece and the tool. The workpiece was meshed with 8000 iso-parametric quadrilateral elements, while the tool modelled as rigid was meshed and subdivided into 1000 elements. A plane-strain coupled thermo-mechanical analysis was performed using orthogonal assumption.

## 2.2. Material Modeling

To model the thermo-visco plastic behaviour of titanium alloy Ti6Al4V, the Johnson–Cook constitutive equation was employed which can be represented by Equation 1 (Umbrello, 2018):

$$\sigma = [A + B(\varepsilon)^n][1 + C \ln \frac{\dot{\varepsilon}}{\dot{\varepsilon}_0}][1 - \left(1 + \frac{T - T_0}{T_{melt} - T_0}\right)^m] \quad (1)$$

where  $\sigma$  is the flow stress,  $\bar{\varepsilon}$  the plastic strain,  $\dot{\varepsilon}$  the strain rate  $s^{-1}$ ,  $\dot{\varepsilon}_0$  the reference plastic strain rate,  $T$  the workpiece temperature,  $T_{melt}$  (1600 °C) the melting temperature of the workpiece material,  $T_0$  (20°C) is the room temperature, coefficient  $A$  (MPa) is the yield strength,  $B$ (MPa) the hardening modulus,  $C$  the strain rate sensitivity coefficient,  $n$  the hardening coefficient,  $m$  is the thermal softening coefficient. In particular, the material Johnson-Cook constants (Table 1) were found under a constant strain rate of 2000  $s^{-1}$  within the temperature range 700–1100°C and a maximum true plastic strain of 0.3. The room temperature was also considered in order to determine the basic mechanical properties.

Table 1: Material Johnson-Cook constants (Stevenson and Wright, 1983)

A (MPa)	B (MPa)	C	n	M	$\dot{\varepsilon}_0 (S^{-1})$
782.7	498.4	0.028	0.28	1	$10^{-5}$

## 2.3. Fracture Criterion and Friction Tool/Chip Interface

In this research, Cockroft and Latham's criterion was employed to predict the effect of tensile stress on the chip segmentation during orthogonal cutting (Umbrello, 2018). Cockroft and Latham' criterion is expressed in Equation 2.

$$\int_0^{\varepsilon_f} \sigma_1 d\varepsilon = D \quad (2)$$

Where  $\varepsilon_f$  is the effective strain;  $\sigma_1$  the maximum principal stress;  $D$  is a material constant. Cockroft and Latham's criterion says that when the integral of the largest tensile principal stress component over the plastic strain path reaches the value of  $D$ , usually called damage value, fracture occurs or chip segmentation starts (Equation 2). In particular, the critical damage value was calculated for each element under deformation at each time-step by the program (Umbrello, 2018). Once the damage value in an element reaches the critical one, a crack is initiated in two steps:

- i. This element is deleted with all the parameters related to it, including element connectivity definition, the strain and stress values
- ii. The rough boundary produced by element deletion is smoothed by cutting out the considered rough angle and adding new points.

Moreover, the utilized software in this research permits applying the fracture criterion by two different techniques, namely; Remeshing–re-zoning methodology and Element Deletion Feature (Sima and Özel, 2010). As far as friction modeling is concerned, a simple model based on the constant shear hypothesis,  $\tau = \mu \tau_0$ , was implemented in the FE-code,  $\tau$  the shear stress,  $\mu$  the friction factor and  $\tau_0$  the shear yield stress. The shear yield stress was obtained as:  $\tau_0 = \sigma_0 / \sqrt{3}$ . This assumption was based on recent investigation where

cutting forces and chip morphology can be well predicted setting the correct friction coefficient independently of which friction law was taken into account (Strenkowski and Moon, 2017).

#### 2.4. FEA Model Verification

In this study, the simulated cutting conditions to verify FEA model was identical to those of the experiments and simulations performed by (Umbrello, 2018) which consists of dry orthogonal cutting of Ti6Al4V alloy at cutting speeds of 60 and 120 m/min, feed rate of 0.12 mm and depth of cut of 2.5mm. Moreover, the Dand  $\mu$  values verified by for Ti-6Al-4V alloy were 245 and 0.7 respectively. The cutting tool geometry for WC ISO-P20 consisted of a normal rake angle and a normal flank angle of 15° and 6° respectively. The tool cutting edge angle was 90°, the tool cutting edge inclination angle was 0° and the tool cutting edge radius was 0.030mm. The reliability of FEA model developed was furtherly investigated for cutting parameters (feed rate and cutting speed) effects on cutting force using percentage error (Equation 3).

$$\text{Percentage Error} = \frac{\text{Experimental Cutting Force} - \text{Predicted Cutting Force}}{\text{Experimental Cutting Force}} \times 100\% \quad (3)$$

#### 2.5. Central Composite Design

The necessary data for building the response models was collected using central composite design (CCD). The factorial portion of CCD was a full factorial design with all combinations of the factors at two levels (high, +1 and low, -1). The design also composed of the four star points and four central points (coded level 0 which is the midpoint between the high and low levels). Table 2 shows the levels of two machining parameters and their ranges. The experimental plan was carried out using the stipulated conditions and involved 12 runs as shown in Table 3. The design was generated and analyzed using Design Expert statistical package.

Table 2: Design scheme of machining parameters and their levels

Parameters	Unit	$-\alpha$	-1	0	+1	$+\alpha$
Cutting speed ( $V_c$ )	m/min	47	60	90	120	132
Feed rate(f)	mm/rev.	0.10	0.12	0.18	0.24	0.26

#### 2.6. Optimisation using Response Surface Methodology

The cutting speed, feed rate are the orthogonal cutting variables selected for this investigation. The experiments were planned by means of Central Composite Design (CCD). The optimum value of the force was obtained using response surface methodology. The Yate's algorithm described by Montgomery (1984) was used to determine the sums of squares of the various sources of variation. The full factorial design formed the basis for the augmentation process through which the Central Composite Design (CCD) was built and thereby used to determine the effects process parameters for the q model developed.

### 3. RESULTS AND DISCUSSION

Table 3 shows the design layout and FEA simulation results while Table 4 shows the experimental and predicted cutting force at different cutting speed and feed rate. Table 4 shows the values of the percentage error obtained by comparing the experimental and predicted values at different cutting speed and feed rate, and it ranges from 0.5% to 5%, these values compared favourably with the values obtained by Umbrello (2018) with percentage error which ranges from 4.3% to 8.2%.

Table 3: Design layout and FEA simulation results

Run number	Cutting speed (V <sub>c</sub> )	Feed rate (f)	Cutting force (F)
1	60	0.12	710.14
2	120	0.12	679.77
3	60	0.24	1378.29
4	120	0.24	1278.49
5	47	0.18	1073.43
6	132	0.18	982.64
7	90	0.10	599.87
8	90	0.26	1341.59
9	90	0.18	978.22
10	90	0.18	1005.63
11	90	0.18	968.09
12	90	0.18	981.88

Table 4: Experimental and predicted cutting force at different cutting speed and feed rate

Run number	Cutting speed (m/min)	Feed rate (mm/rev)	Cutting force (N) (Experimental)	Cutting force (N) (Predicted)	Percentage error (%)
1	30	0.10	712.78	677.14	5
2	40	0.12	772.98	762.93	1.3
3	50	0.14	876.79	848.73	3.2
4	60	0.16	974.47	934.52	4.1
5	70	0.18	1025.44	1020.31	0.5
6	80	0.20	1122.94	1106.10	1.5
7	90	0.22	1213.74	1191.89	1.8
8	100	0.24	1250.19	1277.69	-2.2
9	110	0.26	1412.93	1363.48	3.5
10	120	0.28	1512.81	1449.27	4.2
11	130	0.30	1507.92	1535.06	-1.8
12	30	0.30	1603.57	1642.06	-2.4
13	40	0.28	1583.97	1534.87	3.1
14	50	0.26	1434.85	1427.68	0.5
15	60	0.24	1331.14	1320.49	0.8
16	70	0.22	1266.48	1213.29	4.2
17	80	0.20	1120.67	1106.10	1.3
18	90	0.18	1027.69	998.91	2.8
19	100	0.16	867.43	891.72	-2.8
20	110	0.14	810.47	784.53	3.2
21	120	0.12	677.33	677.33	-2
22	130	0.10	570.14	570.14	2.6

### 3.1. ANOVA Results

#### 3.1.1. FEA model developed

In this study, a hybrid approach of FEA model and Response Surface Methodology was utilized in order to model the effect of cutting parameters on main cutting force of Ti6Al4V alloy. The backward elimination process was used to eliminate the insignificant terms so as to adjust the fitted linear models. These insignificant model terms can be removed and it also displays that the test of lack-of-fit was insignificant. Through the backward elimination process, the final FEA linear model of cutting force equation in terms of actual factors is presented as (Equation 4).

$$F = 4824.61 f - 1.07V_c + 226.78 \quad (4)$$

Where F is cutting force, f the feed rate and  $V_c$  is the cutting speed

### 3.1.2. ANOVA (Analysis of variance)

The statistical significances of the fitted linear model for the cutting force (F) was evaluated by ANOVA, and the result is shown in Tables 5 and 6. When the values of Prob. > 'F' in Table 5 for the term of models are less than 0.05 (i.e.  $\alpha = 0.05$ , or 95% confidence), it indicates that the obtained model terms were considered to be statistically significant, which is desirable, as it demonstrates that the terms in the model have a significant effect on the responses. The coefficient of determination ( $R^2$ ) is a measure of the degree of fit of the model. The closer the  $R^2$  approaches to unity, the better the response model fits the actual data. Furthermore, the value of adequate precision (AP) in this model, which compares the range of the predicted value at the design point to the average prediction error, was well above which means adequate model discrimination. The model obtained present a high value of the coefficient of determination ( $R^2$ ) and adequate precision (AP) at the same time. These values were obtained as follows:  $R^2 = 0.98$  and AP = 43.54 for the model (Table 5). Consequently, these obtained models can be regard as having significant effects for fitting and predicting the experimental results. It also shows that the lack-of-fit was insignificant for the effects. Tables 7 shows that the significant and standard errors of each coefficient for the fitted models, which were also determined by values of; F-value and Prob.> F. As can be seen both cutting force and feed rate can be regards as significant terms due to their Prob. > F value being less than 0.05.

Table 5: ANOVA table for the fitted cutting force model

Sources	Sum of squares	Degree of freedom	Mean square	F-value	Prob>F
Model	678732.4	2	339366.2	239.99	<0.001
Lack of fit	11998.82	6	1999.804	8.24	0.0558
Residual	12726.45	9	1414.05		
Pure error	727.62	3	242.5418		
Cor total	691458.9	11			

Table 6: Fitness parameters for cutting force model

Parameters	Values
Standard deviation	37.60
Mean	998.25
Coefficient of variation	3.76
Predicted residual error of sum of square (PRESS)	26965.62
$R^2$	0.98
$R^2$ adjusted	0.97
Predicted $R^2$	0.961
Adequate precision (AP)	43.54

Table 7: Results of the analysis of variance for the cutting force (F)

Source	Sum of squares	Degree of freedom	Mean square	F-value	Prob>F
Cutting speed	8356.225	1	8356.225	5.909427	0.0379
Feed rate	670376.2	1	670376.2	474.0824	<0.0001
Residual	12726.45	9	1414.05		
Total	691456.9	11			

### 3.2. Effects of Machining Parameters on Cutting Force

Figure 1 shows the response surface of cutting force according to change of cutting speed and feed rate. Feed rate had the highest contribution to the cutting force model. This can be seen from the response surface of the fitted model. Feed rate increase had proportional effect on the cutting force due the increase of unreformed chip thickness and tool load (Miller and Bieler, 1999).

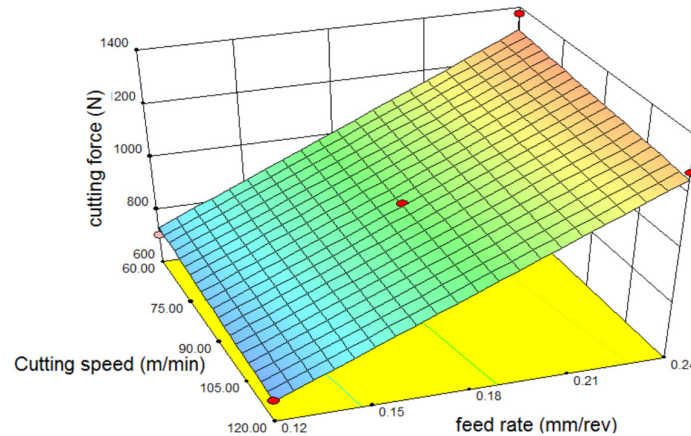


Figure 1: Response surface of cutting force ( $f$ ) according to change of cutting speed and feed rate

It can also be noticed from Figure 1 that increase of cutting speed results in reduction of cutting force due to the increase of shear plane angle and reduction of chip thickness. The lowest cutting force was obtained at highest cutting speed and lowest feed rate level. This tends to reduce the friction force between the chip-tool contacts on the rake face (Kilickap and Huseyinoglu, 2011). The optimum cutting force obtained was 1165.04N at cutting speed of 70m/min and feed rate of 0.21m/rev respectively. These results compared favourably with the result obtained by Özel and Sima (2010) with an optimum cutting force of 1200N at cutting speed of 63m/min and feed rate of 0.18m/rev respectively. The results from this study show that the feed rate had the highest contribution to the fitted model while cutting speed effect was just significant. Figures 2-3 show the chip morphology of deformed chip at the highest and lowest level of cutting speed in which the maximum chip thickness was 0.30mm and 0.26 mm for cutting speed of 47m/min and 132 m/min respectively (Olodu, 2018). These values serve as a guide for this study.

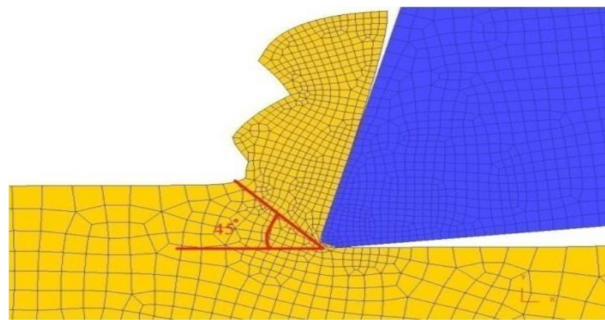


Figure 2: Chip morphology of deformed chips at feed rate of 0.18 mm/rev and cutting speed of 47 m/min (Olodu, 2018)

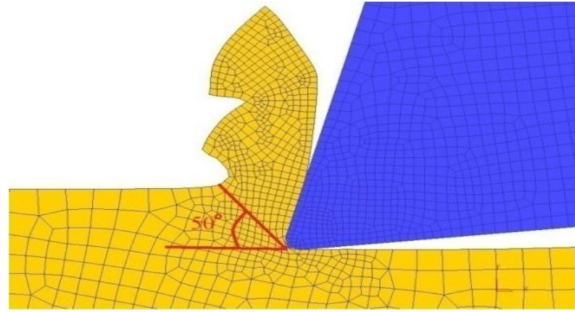


Figure 3: Chip morphology of deformed chips at feed rate of 0.18 mm/rev and cutting speed of 132 m/min (Olodu, 2018)

### 3.3. Confirmation Runs

The five confirmation runs were simulated in order to compare with the predicted values by fitted model and verify the adequacy of the model (Equation 3). The results of the confirmation runs and their comparisons with the predicted values for the cutting force (F) are presented in Table 8. The results of Table 7 revealed a small percentage error. The percentage error was in the range of 0.50% to 5.7%. All the simulated values of confirmation runs were within the 95% prediction interval. This shows that the mathematical model developed was excellently accurate (Equation 4).

Table 8: Results of confirmation runs

Run No.	Cutting speed (m/min)	Feed rate (mm/rev)	Simulated cutting force (N)	Predicted cutting force (N)	Percentage error (%)
1	100	0.18	1049.04	988.20	-5.7
2	80	0.14	797.03	816.62	2.4
3	110	0.14	788.57	784.52	-0.5
4	105	0.21	1092.91	1127.47	3.1
5	70	0.21	1174.99	1165.04	-0.8

### 4. CONCLUSION

In this study, a hybrid approach of FEA model and response surface methodology was utilized in order to model the effect of cutting parameters on main cutting force of Ti6Al4V alloy. The adjusted parameters were good enough for FEA model to simulate the cutting mechanism of Ti6Al4V alloy with reasonable adequacy. The fitted model was able to predict the main cutting force in terms of cutting speed and feed rate with 98% adequacy in the range of selected parameters. Optimum cutting force of 1165.04N was obtained at cutting speed of 70m/min and feed rate of 0.21m/rev. Feed rate had the highest contribution to the fitted model while cutting speed effect was just significant. The lowest cutting force was obtained at highest cutting speed and lowest feed rate level.

### 5. ACKNOWLEDGMENT

The authors wish to acknowledge the assistance and contributions of the staff of the Department of Production Engineering, University of Benin, Benin City toward the success of this research.



## 6. CONFLICT OF INTEREST

There is no conflict of interest associated with this work.

## REFERENCES

- Attanasio, A.E. and Ceretti, D. (2017). Investigation of FEM-based Simulation of Tool Wear in Turning Operations with Uncoated Carbide Tools. *International Journal of Modern Technology*, 269(6), pp. 344-350
- Calamaz, M.J. and Limido, V. (2016). Toward a Better Understanding of Tool Wear Effect Through a Comparison Between Experiments and SPH Numerical Modelling of Machining Hard Materials. *International Journal of Refractory Metals and Hard Materials*. 27(3), pp. 595-604
- Kilickap, E. and Huseyinoglu, M. (2011). Optimization of Drilling Parameters on Surface Roughness in Drilling of AISI 1045 Using Response Surface Methodology and Genetic Algorithm. *International Journal of Advanced Manufacturing Technology*, 52(4), pp. 79-88
- Miller, R.M. and Bieler, T.R. (1999). Flow Softening During Hot Working of Ti–6Al–4V with a Lamellar Colony Microstructure. *Journal of Scripta Materialia*, 40(12), pp. 1387–1393
- Olodu, D.D. (2018). Optimization and Analysis of Cutting Tool Geometrical Parameters Using Taguchi Method. *Journal of Applied sciences and Environmental Management*, 22(3), pp. 346-349
- Özel, T. and Sima, M. (2010). Investigations on the Effects of Multi-Layered Coated Inserts in Machining Ti–6Al–4V Alloy with Experiments and Finite Element Simulations. *Journal CIRP Annals-Manufacturing Technology*, 59(1), pp. 77-82.
- Sartkulvanich, P. and Altan, T. (2016). Effects of Flow Stress and Friction Models in Finite Element Simulation of Orthogonal Cutting; A Sensitivity Analysis. *Journal of Machining Science and Technology*, 9(1), pp. 1-26
- Sasahara, H. (2005). The Effect on Fatigue Life of Residual Stress and Surface Hardness Resulting from Different Cutting Conditions of 0.45%C Steel. *International Journal of Machine Tools and Manufacture*, 45(2), pp. 131-136
- Sima, M. and Özel T. (2010). Modified Material Constitutive Models for Serrated Chip Formation Simulations and Experimental Validation in Machining of Titanium Alloy Ti–6Al–4V. *International Journal of Machine Tools and Manufacture*, 50(1), pp. 943-960
- Stevenson, M.G. and Wright, P.K. (1983). Further Development in Applying the Finite Element Method to the Calculation of Temperature Distribution in Machining and Comparison with Experiment. *Journal of Engineering for Industry*, 105, pp. 149–154
- Strenkowski, J.S. and Moon, K.J. (2017). Finite Element Prediction of Chip Geometry and Tool/Workpiece Temperature Distributions in Orthogonal Metal Cutting. *ASME Journal of Engineering for Industry*, 152, pp. 313–318
- Umbrello, D. (2018). Finite Element Simulation of Conventional and High Speed Machining of Ti6Al4V alloy. *Journal of Materials Processing Technology*, 207(1–3), pp. 79-87.